

# Relationship between mitral annulus function and mitral regurgitation severity and left atrial remodelling in patients with primary mitral regurgitation

Sorina Mihaila<sup>1,2\*</sup>, Denisa Muraru<sup>1</sup>, Marcelo Haertel Miglioranza<sup>1,3</sup>, Eleonora Piasentini<sup>1</sup>, Patrizia Aruta<sup>1</sup>, Umberto Cucchini<sup>1</sup>, Sabino Iliceto<sup>1</sup>, Dragos Vinereanu<sup>2</sup>, and Luigi P. Badano<sup>1</sup>

<sup>1</sup>Department of Cardiac, Thoracic and Vascular Sciences, University of Padua, Via Giustiniani 2, CAP 35128 Padua, Italy; <sup>2</sup>University of Medicine and Pharmacy 'Carol Davila', Bucharest, Romania; and <sup>3</sup>Cardiology Institute of Rio Grande do Sul, Porto Alegre, Brazil

Received 2 March 2015; accepted after revision 9 August 2015; online publish-ahead-of-print 12 January 2016

## Aims

To explore the relationship between the mitral annular (MA) remodelling and dysfunction, mitral regurgitation (MR) severity, left ventricular (LV) and atrial (LA) size and function in patients with organic MR (OMR).

## Methods and results

A total of 52 patients ( $57 \pm 15$  years, 31 men) with mild to severe OMR and 52 controls underwent 3D transthoracic echocardiography acquisitions of the mitral valve (MV), LA, and LV. MA geometry and dynamics, LV and LA volumes, LV ejection fraction (LVEF) and emptying fractions (LAEF) were assessed using dedicated software packages. LA and LV myocardial deformations were assessed using 2D speckle-tracking echocardiography. OMR patients presented larger and more spherical MA than controls during the entire systole ( $P < 0.001$ ). Although the MA non-planarity at early-systole was similar between OMR and controls ( $157 \pm 13^\circ$  vs.  $153 \pm 12^\circ$ ,  $P = \text{NS}$ ), the MA became flatter from mid-to end-systole ( $153 \pm 12$  vs.  $146 \pm 10^\circ$  and  $157 \pm 12$  vs.  $147 \pm 8^\circ$ ,  $P < 0.01$ ) in OMR. MA area fractional change was lower in patients with OMR ( $22 \pm 5\%$  vs.  $28 \pm 5\%$ ,  $P < 0.001$ ), and correlated with the MR orifice and volume ( $r = -0.52$  and  $r = -0.55$ ). MA fractional area change correlated with LA minimum and maximum volumes ( $r = 0.77$  and  $r = 0.70$ ), total and active LAEF ( $r = 0.72$  and  $r = 0.76$ ), and LA negative strain and strain rate ( $r = 0.52$  and  $r = 0.57$ ), but not with the LVEF or LV global longitudinal strain. In a multivariate regression model using LAEF and LVEF, solely active LAEF correlated with the MA fractional area change ( $\beta = 0.51$ ,  $P = 0.005$ ).

## Conclusion

In patients with OMR, MA reduced function correlates with the MR severity and the LA size and function, but not with the LV function.

## Keywords

mitral annulus dysfunction • organic mitral regurgitation • three-dimensional echocardiography • transthoracic echocardiography • mitral valve

## Introduction

Degenerative disease is the most common form of organic mitral valve (MV) disease in developed countries,<sup>1</sup> and the second most common valvular lesion needing cardiac surgery.<sup>2</sup> It is most frequently associated with MV prolapse (MVP) due to fibro-elastic deficiency and the Barlow disease,<sup>1</sup> characterized by leaflet redundancy and chordae elongation. Besides heart failure symptoms and

mitral regurgitation (MR) severity, important factors also associated with progression of the disease are the left ventricular (LV) size and function, the development of atrial fibrillation, and the increase of pulmonary pressures, currently used for risk stratification and surgical decision. However, recent studies have revealed that left atrial (LA) and mitral annulus (MA) remodelling and dysfunction might also have prognostic implication in organic MR (OMR).<sup>3–5</sup> LA function has been proposed as an additional tool to guide the optimal

\* Corresponding author. Tel: +39 049 8218640; Fax: +39 049 8211802. E-mail: sorinamihaila@yahoo.com

timing of surgery for MVP.<sup>6</sup> New three-dimensional transthoracic echocardiography (3DE) techniques and dedicated software for MV quantitative analysis revealed that patients with moderate-severe OMR also present remodelling and dysfunction of the MA.<sup>3–5</sup> However, the presence of MR was associated with MA dilation and flattening in patients with MVP,<sup>3</sup> but the relation between the dysfunction of the MA and the severity of MR has not been assessed yet. Moreover, in patients with ischaemic MR, it has been proposed that enlargement of the LA has the potential to increase mitral leaflet tethering and worsen MR through a mechanism unrelated to LV remodelling.<sup>7</sup> However, in patients with OMR, the relation between the size and function of the MA and the size and function of LA and LV remains to be clarified.

Thus, we hypothesized that, in patients with OMR, the reduced function and the altered geometry of the MA are associated to the severity of the MR, and they are more related to LA than to LV remodelling.

## Methods

### Study population

Between January 2013 and January 2014, we enrolled 52 consecutive patients ( $57 \pm 15$  years, 31 males) with mild to severe OMR due to simple or complex forms of MVP (40 patients) or the Barlow disease (12 patients) and 52 healthy volunteers matched for age, gender, and body size. All study subjects were in regular rhythm. Patients with more than mild aortic, tricuspid or pulmonary valve diseases, severe MV calcification, history of coronary artery disease, and poor apical acoustic window were excluded from the study.

Control subjects inclusion criteria were: age  $>17$  years, no history or symptoms of cardiovascular or lung disease, no cardiovascular risk factors, normal ECG, and no cardio- or vasoactive treatment. Exclusion criteria were trained athletes, pregnancy, body mass index  $>30$  kg/m<sup>2</sup>, and poor apical acoustic window.

Blood pressure, height, and weight were measured, and body surface area (BSA) was calculated in all subjects. An ECG was performed to confirm sinus rhythm in all subjects, and to exclude electrical abnormalities in healthy volunteers. University of Padua Ethics Committee approved the study (Protocol 2380 P), and all subjects provided an informed consent.

### Echocardiography

Using a standardized acquisition protocol, all examinations were performed using commercially available Vivid E9 system (GE Vingmed Ultrasound, Horten, Norway) equipped with M5S and 4 V probes. First, standard transthoracic echocardiography was performed to assess the aetiology and severity of the MR in patients with degenerative MV disease, and to exclude subclinical heart diseases in control subjects. Three consecutive cycles were recorded at a frame rate between 60 and 80 fps during breath hold with stable ECG tracing to obtain suitable apical views for the LA and LV two-dimensional (2D) speckle-tracking analysis.<sup>8,9</sup>

Then, three separate full-volume multi-beat 3D datasets of the MV, LV, and LA were acquired by combining six consecutive ECG-triggered sub-volumes to obtain high temporal resolution. Acquisitions were performed during patient's breath holding and avoiding patient or probe movement in order to obtain datasets free of stitching artefacts. Care was taken to encompass the MV and the entire LV and LA cavities in the datasets.

### Image analysis

In patients with OMR, the MVP was defined by the displacement of more than 2 mm of one of the MV leaflet below the MA plane<sup>1</sup> and the differentiation between MVP and the Barlow disease was made using both 2D and 3DE morphological assessments of the MV leaflets.<sup>10</sup> A leaflet was considered flail when the leaflet edge was pointing retrograde into the LA at end-systole, whether or not ruptured chordae were seen.<sup>11</sup> The MR severity was graded from mild to severe using both 2DE qualitative and quantitative assessment according to the current guidelines.<sup>12</sup> Mitral regurgitant jet vena contracta, proximal isovelocity surface area (PISA) radius, effective regurgitant orifice area (EROA), and regurgitant volume (RVol) were measured.

### Quantitative analysis of left cardiac chambers geometry and function

2D and 3DE datasets of the LV were stored digitally in raw-data format for offline analysis using commercially available software package (EchoPAC BT 12, GE Vingmed Ultrasound, Horten, Norway). Quantification of 3D LV volumes and LV ejection fraction (LVEF) was performed using 4D Auto-LVQ option, as previously described and validated against cardiac magnetic resonance.<sup>13</sup> LV myocardial deformation in the longitudinal, radial and circumferential components was assessed using 3D speckle-tracking analysis to measure global LV longitudinal (GLS), radial (GRS), circumferential (GCS), and area (GAS) strain, as previously described.<sup>13</sup>

3DE full-volume datasets of the LA were converted to DICOM format and analysed using dedicated software designed for volumetric analysis of the LA, recently validated against cardiac magnetic resonance (LA analysis 2.3, TomTec Imaging Systems, Unterschleissheim, D).<sup>14</sup> As previously described,<sup>14</sup> the maximum (LAVmax), minimum (LAVmin), and pre-atrial contraction (LAVpreA) volumes of the LA were measured. Then, using the LA volumes, the software automatically assessed the active, passive, and total LA emptying fractions<sup>14</sup> (Figure 1).

2DE datasets dedicated for the LA were digitally stored for offline analysis of LA myocardial function, using Q-analysis option (EchoPAC BT 12, GE Vingmed Ultrasound). The LA endocardium was manually traced when the LA was at its minimum volume after contraction<sup>9</sup> and a peak global longitudinal atrial strain (LAS) curve was automatically generated which included a negative deflection (negative LAS), representing LA active contraction, followed by a positive one (positive LAS) during LA filling. The summation of negative and positive LAS was recorded as total LAS. Using the same cine-loop, the software automatically displays the strain rate (SR) curve of the LA. The positive peak during LA filling (positive LASR), early negative peak during early LV filling (early negative LASR), and the late negative peak during the atrial contraction (late negative LASR) were also recorded.<sup>9</sup>

### Quantitative analysis of the mitral annulus

3DE MV datasets were converted to DICOM format and analysed using dedicated software for MV quantitative analysis (4D-MV assessment 2.3, TomTec Imaging Systems, Unterschleissheim, D), as previously described.<sup>15</sup> Mitral annulus analysis started by identifying three time points: early-systole—the frame after the MV closure (MVC); end-systole—the frame just before MV starts to open; and mid-systole—the frame midway between MVC and end-systole. After adding anatomical landmarks for the MA, aorta, and leaflet coaptation point, the software created a static 3D model of the MA and leaflets at mid-systolic frame (*static analysis*) (Figure 2). Afterwards, the MA was tracked in each frame of the cardiac systole (*dynamic analysis*) (Figure 2). Manual edits of the dynamic models were performed as needed. Quantitative parameters of MA geometry were as follows: MA 3D and 2D (projected) areas; MA circumference; anteroposterior (AP) and anterolateral-posteromedial

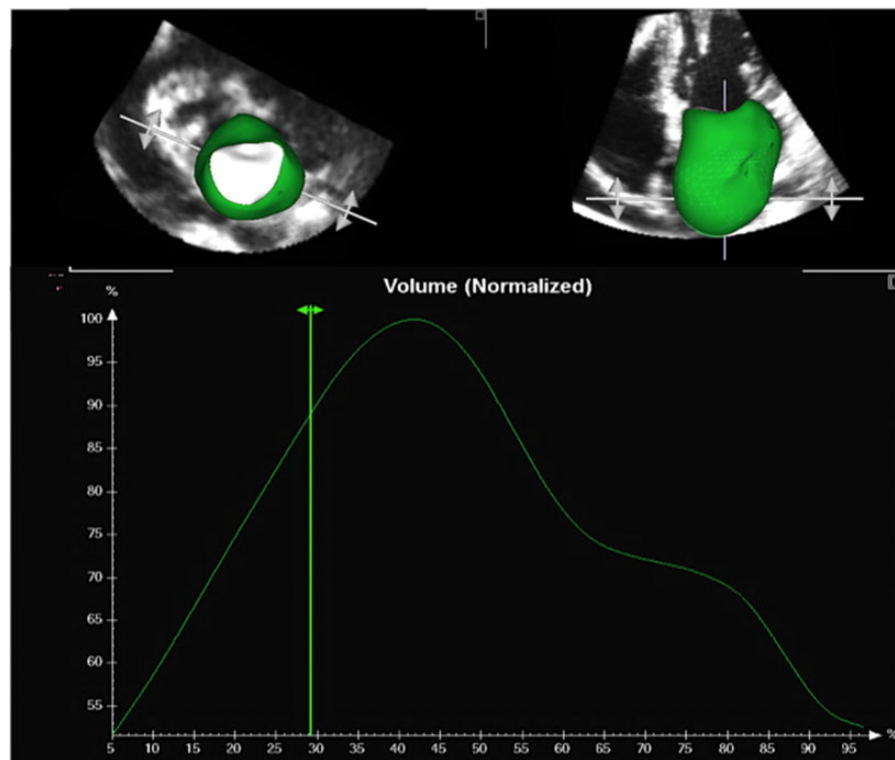


**Figure 1** Left atrium analysis using 3D echocardiography and dedicated software. LA phasic volumes and emptying fractions are automatically measured, after tracking the endocardium in three standard 2D views obtained by slicing the 3D dataset of the left atrium.

(AL-PM) diameters; MA sphericity index; MV commissural diameter; anterior leaflet area (ALA) and length; posterior leaflet area (PLA) and length; the non-planarity angle of the MA; MV annular height; MV tenting height, area, and volume; and Ao-AP angle. For all quantitative parameters, the values at MVC, mid-systole and end-systole, and the minimal value have been recorded. In addition, we recorded the time interval from the MVC to the moment of its minimal value expressed as percentage (%) of the total duration of the systole. MA diameters, area, and circumference were indexed by patients' BSA.

The software provided also the MA displacement, displacement velocity, and fractional area change. In addition, the fractional change (difference between the maximal and minimal value, divided by the maximal value, and expressed as percentages, %) of MA circumference, AP, and AL-PM diameters were also calculated.

### Statistical analysis

Normal distribution of variables was checked by the Kolmogorov–Smirnov test. Continuous variables were summarized as mean  $\pm$  SD, and categorical variables were reported as percentages. Variables were compared between groups using paired *t*-test. Two-way ANOVA for repeated measures test was used to assess the dynamic changes of the MA parameters at each reference-point of the cardiac cycle. In patients with OMR, Pearson's correlation was used to analyse the relationships between MR severity parameters and MA function indexes, and between MA function indexes and parameters of LA and LV size and function. Multiple linear stepwise regression tests were used to identify the parameters that independently correlated to the MA reduced function in the group with OMR, by introducing in the models only parameters that were related to the MA fractional area change.

Inter-observer variability for MA assessment using 3DTTE was performed in 17 random healthy subjects by two independent observers by blinded offline analysis of the same 3D dataset, as previously reported.<sup>15</sup> One observer repeated the measurements of the same datasets 7 days later, to assess the intra-observer variability. Reproducibility was reported as intra-class correlation coefficient (ICC).

All analyses were carried out using SPSS version 20.0 (SPSS, Inc., Chicago, IL) and MedCalc version 10.0.1.0 (MedCalc Software, Mariakerke, Belgium). Differences among variables were considered significant at  $P < 0.05$ .

## Results

### Study population's characteristics

Demographics and general characteristics of the 52 patients (age range 17–85 years, 60% males) and 52 controls enrolled in the study are summarized in Table 1. Two patients with OMR were excluded from the initial lot of 58 due to advanced age (difficulty of finding matched control), and 4 of them due to poor quality image of the 3DE MV dataset. The remaining 52 patients with OMR presented anterior or posterior leaflet prolapse (40 patients) or the Barlow disease (12 patients). Among them, 14 patients were found to have MV leaflet flail, and 38 had MV leaflet prolapses without flail.

In patients with OMR, PISA radius could be measured in 45 (87%), RVol could be calculated in 30 (58%), and EROA in 27 (52%). In the remaining patients, the quantitative parameters for MR severity could not be measured because they had milder degrees of MR.

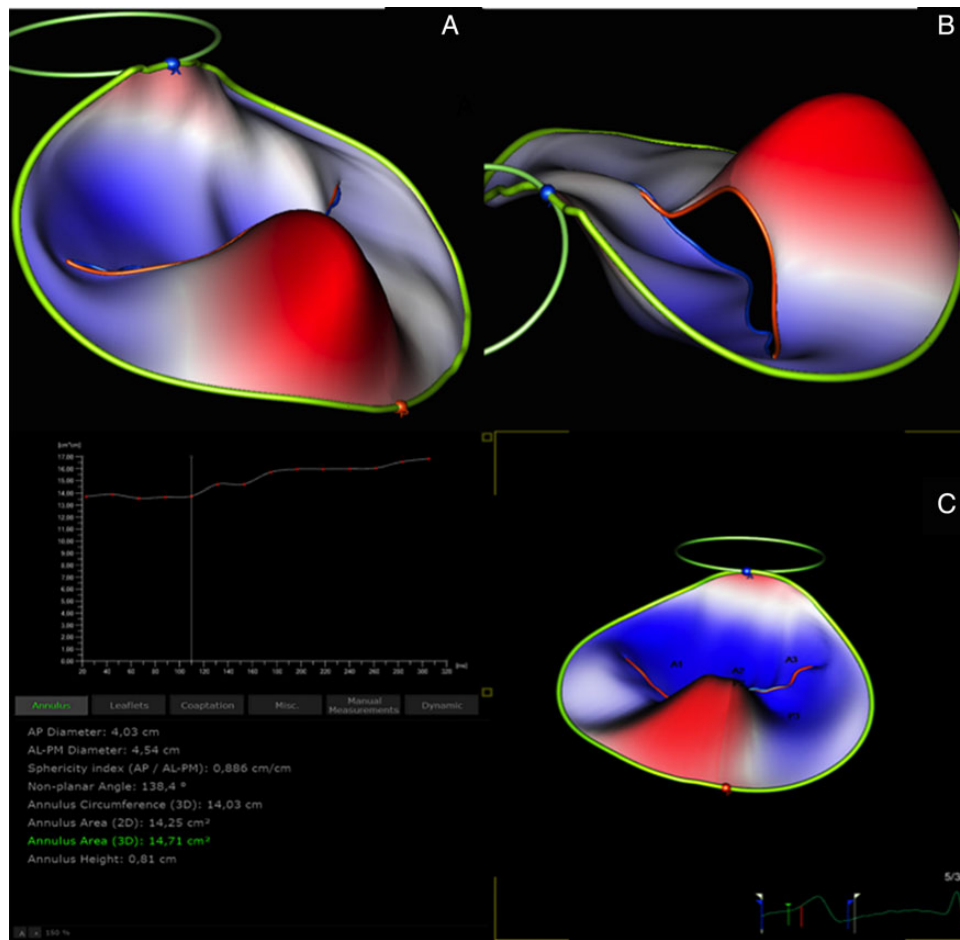


**Figure 2** Static (A and B) and dynamic analysis (C) of the MA area using 3D echocardiography and dedicated software in patient with MVP. The MA area change during the cardiac systole is computed and a curve for its dynamics is afterwards provided. The prolapse of the P2 scallop is coloured by the software in red.

According to current recommendations for the assessment of OMR severity, 50% of our patients had severe MR (Table 1).

Even though patients with OMR presented larger LV volumes than controls, the LVEF was similar in the two groups (Table 1). Three-dimensional LV GLS was also similar between patients with OMR and controls ( $18.3 \pm 3$  vs.  $18.6 \pm 4\%$ ,  $P > 0.05$ ). As expected, patients with OMR had dilated LA (Table 1).

The temporal resolution and feasibility of quantitative analysis of the 3D datasets and speckle-tracking analysis was summarized in Table 2. The number of systolic frames in each 3D dataset dedicated for the MA analysis ranged from 11 to 21, depending on patient's heart rate or acquisition settings and did not differ between patients with OMR and controls.

### Mitral annulus analysis in patients with organic mitral regurgitation compared with controls

When compared with controls, patients with OMR presented larger MA diameters, area and circumference during the entire cardiac systole

(Table 3, Figure 3). At the MVC, the MA area was 37% larger in patients with OMR. While ALA was similar between patients with OMR and controls, the PLA was larger in patients with OMR, leading to a significantly decreased ALA/PLA ratio in OMR compared with controls.

Moreover, the times to minimum AP and AL-PM diameter, as well as of minimal MA area and circumference were longer in patients with OMR than in controls (Table 3). Patients with OMR showed more spherical mitral annuli throughout the entire cardiac systole, with a delayed occurrence of minimal MA sphericity.

At MVC, MA non-planarity angle, MV tenting volume and MV tenting area were similar between patients with OMR and control subjects. Conversely, from mid- to end-systole, the non-planarity angle became progressively larger in patients with OMR than in controls. At the same times, the MV tenting area and volume became progressively smaller in OMR than in control subjects (Table 3, Figure 3), due to the MV leaflet prolapse. However, the timing of the minimum non-planarity angle did not differ among groups. At MVC, MV annular height was similar between patients with OMR and controls. However, it became smaller in patients with OMR than in controls from mid- to end-systole.

**Table 1** General characteristics of patients with OMR and control subjects

	OMR patients N = 52	Controls N = 52	P
Age (years)	57 ± 15	56 ± 13	0.78
Gender (males)	31	31	1.0
Heart rate (beats/min)	65 ± 7	73 ± 13	0.001
Systolic blood pressure (mm Hg)	132 ± 20	127 ± 17	0.20
Diastolic blood pressure (mm Hg)	78 ± 10	74 ± 8	0.06
BSA (m <sup>2</sup> )	1.75 ± 0.2	1.82 ± 0.2	0.06
MR severity (%)			
None/trivial	0	100	
Mild	25	0	
Moderate	25	0	
Severe	50	0	
MR effective regurgitant area (cm <sup>2</sup> )	0.47 ± 0.31		
MR regurgitant volume (mL)	63 ± 44		
LV end-diastolic volume (mL/m <sup>2</sup> )	84 ± 21	57 ± 10	<0.001
LV end-systolic volume (mL/m <sup>2</sup> )	33 ± 9	21 ± 5	<0.001
LVEF (%)	60 ± 11	58 ± 19	0.465
LA max volume (mL/m <sup>2</sup> )	62 ± 23	34.7 ± 5	<0.001

LV, left ventricular; MR, mitral regurgitation.

**Table 2** Temporal resolution and feasibility of quantitative analysis of 3D datasets and 2D views for speckle-tracking analysis

	OMR patients (n = 52)	Controls (n = 52)	P
Temporal resolution MV datasets (vps)	40 ± 8	38 ± 8	0.364
Feasibility of static MA analysis (%)	100	98	1.000
Feasibility of dynamic MA analysis (%)	96	90	0.807
Temporal resolution of 3DE LV datasets (vps)	40 ± 7	38 ± 8	0.348
Feasibility of LV volume measurements (%)	98	92	0.808
Feasibility of LV global longitudinal strain (%)	86	96	0.712
Temporal resolution of 3DE LA datasets (vps)	38 ± 11	41 ± 16	0.004
Feasibility of LA volume measurements (%)	77	96	0.386
Temporal resolution of 2DE LA views (fps)	69 ± 8	75 ± 6	0.348
Feasibility of LA global longitudinal strain (%)	80	96	0.535

2DE, two-dimensional echocardiography; 3DE, three-dimensional echocardiography; LA, left atrium; LV, left ventricle; MA, mitral annulus; MV, mitral valve.

MA fractional area change was lower in patients with OMR than in controls (Table 4). AP and AL-PM diameter fractional changes were also reduced in patients with OMR when compared with controls, but more for the AP size than for the AL-PM one. While the MA displacement was similar between groups, the displacement velocity was higher in patients with OMR than in controls.

#### Mitral annulus size and function related to mitral regurgitation severity

MA area from patients with OMR presented significant correlation with PISA radius and EROA ( $r = 0.40$ ,  $P = 0.013$  and

$r = 0.40$ ,  $P = 0.046$ , respectively). PLA also presented a positive correlation with PISA radius ( $r = 0.33$ ,  $P = 0.028$ ). Furthermore, MA fractional area change presented an inverse correlation with all quantitative parameters of MR severity (Figure 4).

#### The relation between mitral annulus and left chambers size and function in patients with organic mitral regurgitation

MA area and circumference measured at mid-systolic frame presented a modest, but significant positive relation to LV end-diastolic and end-systolic volumes ( $r = 0.44$  and  $r = 0.46$ , respectively, both  $P = 0.001$ ) (Figure 5). However, MA fractional area change was not

**Table 3** The dynamic changes of the MV and MA dimensions and geometry in patients with OMR compared with controls, during the cardiac systole

	Early-systole	Minimal value	Mid-systole	End-systole	Time to minim (%)
MV and MA dimensions					
AP diameter (cm)					
OMR	3.4 ± 0.6*	3.2 ± 0.6*	3.6 ± 0.6*	3.8 ± 0.7*	19 ± 12*
Controls	2.4 ± 0.3	2.4 ± 0.3	2.8 ± 0.4	2.9 ± 0.3	11 ± 8
AL-PM diameter (cm)					
OMR	4.3 ± 0.7*	4.2 ± 0.6*	4.6 ± 0.7*	4.7 ± 0.7*	20 ± 13*
Controls	3.5 ± 0.4	3.4 ± 0.3	3.9 ± 0.4	3.9 ± 0.5	13 ± 8
Commissural diameter (cm)					
OMR	4.2 ± 0.7*	4.1 ± 0.6*	4.4 ± 0.7*	4.5 ± 0.7*	26 ± 22*
Controls	3.5 ± 0.4	3.4 ± 0.4	3.8 ± 0.4	3.9 ± 0.4	12 ± 8
MA area 2D (cm <sup>2</sup> )					
OMR	11.7 ± 3.7*	11.3 ± 3.6*	13 ± 3.9*	14.0 ± 4.1*	18 ± 12*
Controls	7.3 ± 1.5	7.0 ± 1.4	8.7 ± 1.8	9.4 ± 1.7	11 ± 6
MA area 3D (cm <sup>2</sup> )					
OMR	11.9 ± 3.7*	11.5 ± 3.6*	13.2 ± 4.0*	14.2 ± 4.2*	18 ± 13*
Controls	7.5 ± 1.5	7.2 ± 1.4	9.0 ± 1.9	9.6 ± 1.8	11 ± 2
MA circumference (cm)					
OMR	12.5 ± 1.9*	12.3 ± 1.9*	13.2 ± 2.0*	13.7 ± 1.9*	16 ± 7*
Controls	10.2 ± 1.0	10.1 ± 1.0	11.1 ± 1.2	11.5 ± 1.1	11 ± 6
ALA (cm <sup>2</sup> )					
OMR	6.5 ± 1.9	6.1 ± 2.0	6.4 ± 2.2	6.5 ± 2.2	47 ± 32
Controls	6.1 ± 1.2	5.7 ± 1.2	6.1 ± 1.4	6.2 ± 1.4	38 ± 33
PLA (cm <sup>2</sup> )					
OMR	7.5 ± 2.6*	7.1 ± 2.8*	8.0 ± 2.8*	8.9 ± 3.3*	27 ± 21
Controls	4.0 ± 1.0	3.7 ± 1.0	3.9 ± 1.0	4.6 ± 1.0	30 ± 25
Anterior leaflet length (cm)					
OMR	2.1 ± 0.4	2.0 ± 0.4	2.1 ± 0.4	2.1 ± 0.4	59 ± 33
Controls	2.2 ± 0.3	2.1 ± 0.3	2.2 ± 0.3	2.2 ± 0.3	48 ± 35
Posterior leaflet length (cm)					
OMR	1.7 ± 0.5*	1.5 ± 0.5*	1.8 ± 0.5*	1.8 ± 0.6*	43 ± 32*
Controls	1.1 ± 0.2	0.9 ± 0.2	1.0 ± 0.2	1.1 ± 0.2	48 ± 30
MV and MA geometry					
Sphericity index					
OMR	0.75 ± 0.09*	0.71 ± 0.07*	0.76 ± 0.07*	0.79 ± 0.07*	38 ± 28*
Controls	0.67 ± 0.06	0.65 ± 0.06	0.72 ± 0.06	0.76 ± 0.06	22 ± 18
Non-planarity angle (°)					
OMR	157 ± 13	147 ± 11*	153 ± 11*	157 ± 12*	48 ± 27
Controls	153 ± 12	141 ± 9	145 ± 10	147 ± 8	54 ± 30
Annular height (mm)					
OMR	5.3 ± 0.2	4.4 ± 0.2*	5.7 ± 0.2*	5.6 ± 0.2*	50 ± 36*
Control	5.5 ± 0.1	5.2 ± 0.1	6.6 ± 0.1	6.3 ± 0.1	30 ± 28
Tenting volume (cm <sup>3</sup> )					
OMR	2.9 ± 1.1	0.8 ± 0.7*	1.3 ± 0.9*	1.2 ± 0.8*	85 ± 12
Control	2.8 ± 1.1	1.3 ± 0.7	1.8 ± 0.7	2.1 ± 0.9	77 ± 14
Tenting area (cm <sup>2</sup> )					
OMR	1.4 ± 0.7	0.5 ± 0.4*	0.8 ± 0.5*	0.7 ± 0.5*	78 ± 19
Control	1.5 ± 0.4	1.0 ± 0.3	1.2 ± 0.3	1.3 ± 0.5	72 ± 23
Tenting height (mm)					
OMR	7.7 ± 2.0	2.6 ± 1.8*	4.6 ± 2.2*	3.2 ± 1.9*	91 ± 10*
Control	8.5 ± 1.4	4.4 ± 1.5	6.2 ± 1.3	6.0 ± 1.9	80 ± 15

Continued

**Table 3 Continued**

	Early-systole	Minimal value	Mid-systole	End-systole	Time to minim (%)
Angle aorta-MA (°)					
OMR	138 ± 12*	136 ± 13*	143 ± 11*	151 ± 13*	21 ± 20
Control	130 ± 11	126 ± 11	132 ± 13	139 ± 13	25 ± 16

Statistically significant with  $P < 0.01$ .  
OMR, organic mitral regurgitation.

significantly related to LV function parameters like LVEF ( $r = 0.2$ ,  $P = 0.2$ ), 3D LV GLS, GCS, or GRS ( $r = 0.3$ ,  $P = 0.6$ ;  $r = 0.1$ ,  $P = 0.7$ ; and  $r = 0.25$ ,  $P = 0.12$ , respectively). Conversely, MA displacement showed a weak positive correlation with the 3D LV GLS ( $r = 0.31$ ,  $P = 0.04$ ).

LA maximum volume correlated with both AP and AL-PM diameters of the MA ( $r = 0.69$  and  $r = 0.50$ , respectively, for both  $P \leq 0.001$ ). LA maximum volume showed a positive correlation with MA area ( $r = 0.63$ ,  $P < 0.001$ ) (Figure 6), with ALA ( $r = 0.53$ ,  $P = 0.001$ ) and with PLA ( $r = 0.55$ ,  $P < 0.001$ ). Furthermore, MA fractional area change presented an inverse correlation with the LA maximum and minimum volumes and a positive correlation with both total and active LA emptying fractions (Figure 6). MA fractional area change correlates with both negative LA strain and SRs, too (Figure 6).

In a multiple stepwise regression model using total and active LA emptying fractions, and minimal and maximal LA volumes, solely the active LA emptying fraction independently related to MA fractional area change ( $\beta = 0.43$ ,  $P = 0.01$ ). Moreover, in a similar model using negative LA strain and SR, solely late negative LA SR independently correlated to MA fractional area change ( $\beta = 0.56$ ,  $P = 0.007$ ).

### Reproducibility

MA parameters obtained by 3DTTE showed excellent intra- and inter-observer reproducibility, with ICCs ranging from 0.87 to 0.98 for intra-observer, and 0.78 to 0.95 for inter-observer reproducibility (Table 5).

## Discussion

Our study provides a complete description of MA remodelling occurring in patients with mild to severe OMR by comparison with normal individuals, and analyses the relation between the function of the MA and MR severity. Furthermore, our study was the first to explore the relationships between LA and LV size and function and the remodelling and dysfunction of the MA in patients with OMR.

The main results of the study are as follows: (1) patients with OMR have increased MA size and altered MA geometry when compared with normal individuals; (2) in patients with OMR, the distortion of the MA geometry progresses from early to late systole by decreasing MA height and non-planarity angle; (3) in patients with OMR, the extent of MA area change during systole is decreased and delayed, but MA translation is preserved; (4) in patients with mild to severe OMR, the extent of MA area change during systole is inversely related to MR severity and it is further reduced in

patients with leaflet flail; and (5) in patients with OMR, MA remodelling and dysfunction correlates with the LA size and function, but not with the LV systolic function.

Degenerative MR is the most common organic MV disease in developed countries,<sup>1</sup> and surgical repair remains the best treatment option for a patient with severe OMR.<sup>16</sup> Even if surgical MV repair was associated with good long-term survival and remained superior to MV replacement for long-term follow-up,<sup>16</sup> degenerative MV disease still has a sizable risk of recurrence of MR after surgery. This seems to be related to the progression of the MV and MA disease.<sup>17</sup> Moreover, one of the predictors for a successful MV repair is the extent of the MA disease.<sup>18</sup> Therefore, thorough assessment of the MA geometry and function and determinants of MA remodelling in OMR have become pivotal to understand the pathophysiology and the severity of OMR, and to plan effective reparative surgery.

Echocardiography guides the timing of surgical intervention by assessing MR severity, monitoring LV and LA remodelling, and estimating pulmonary-artery systolic pressure.<sup>19</sup> Currently, the only recommendation about the echocardiographic assessment of the MA before surgery is the measurement of its AP diameter using the 2DE long axis view of the LV.<sup>20</sup> However, accuracy of 2DE in measuring the AP diameter of the MA depends critically on correct alignment of anatomical landmarks,<sup>21</sup> and it is now widely accepted that the complex 3D and highly dynamic geometry of the MA cannot be comprehensively described by one single linear measurement.

The advent of 3DE, using dedicated software that extracts a realistic model of the MA from the 3D dataset and permits thorough MA quantitative assessment, completely changed our way of assessing MA shape and function. MA quantitative analysis has been used for a better understanding of OMR pathophysiology,<sup>3</sup> and in following up patients.<sup>22</sup> However, MA dynamics in OMR is still controversial,<sup>3–5</sup> the relationship between the function of MA and MR severity has not been reported, and the relation between the remodelling of the MA and left heart chamber size and function remains to be defined.

Increased MA size in patients with OMR has already been documented.<sup>4,5</sup> However, compared with the patients studied by Grewal et al.<sup>4</sup> who showed only persistent increase of the MA commissural diameter, the patients with OMR in our study presented an increase of all MA diameters. Similarly to our findings, Biaggi et al.<sup>23</sup> reported a progressive increase in both AP and AL-PM diameters in patients with OMR. We also found that, due to a disproportionate enlargement in the AP size, the shape MA of patients with OMR was more spherical than in controls.

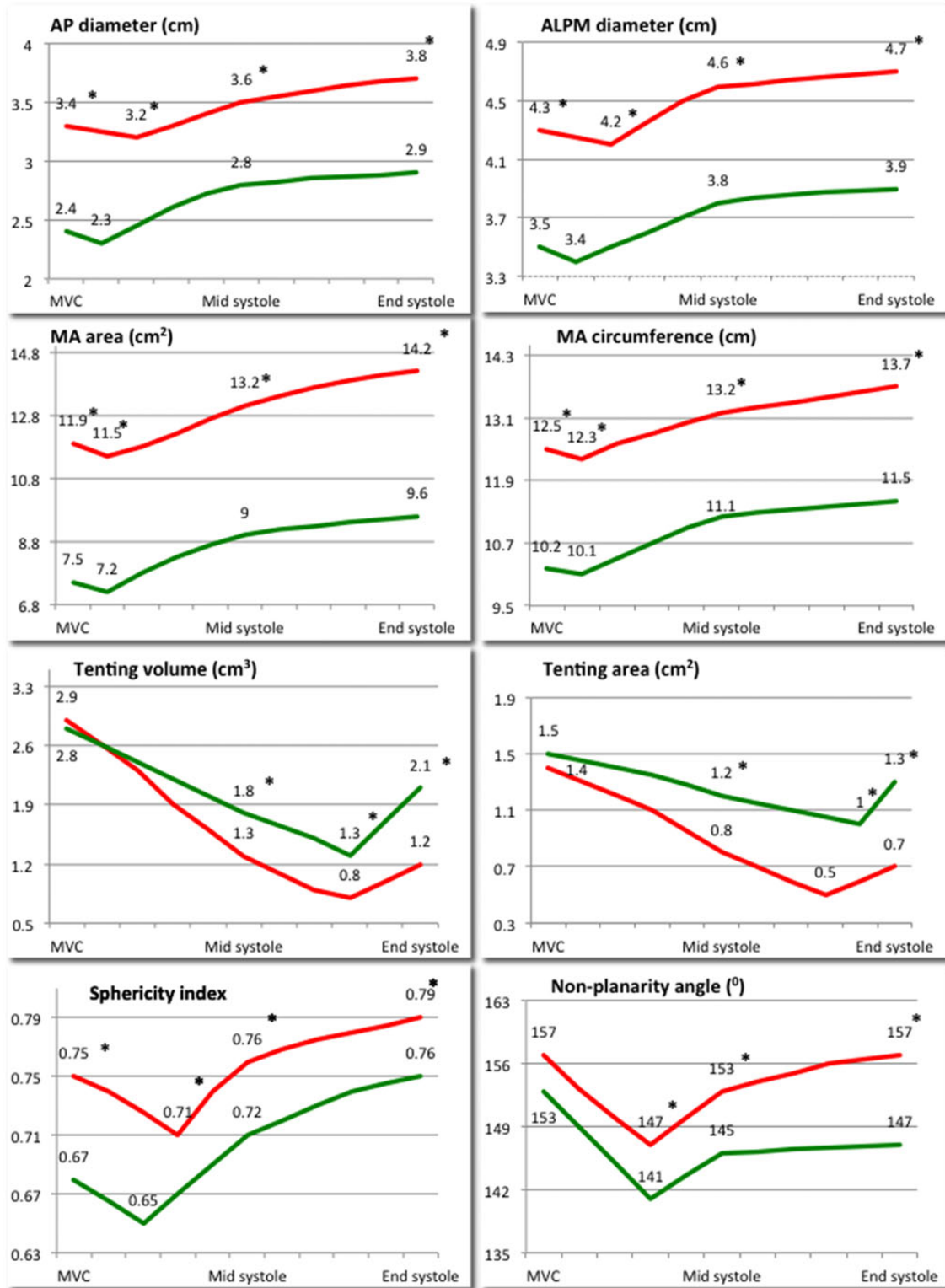


**Figure 3** MA parameters analysed in dynamic during the cardiac systole in patients with OMR and control subjects. AP, anteroposterior; AL-PM, anterolateral-posteromedial; MA, mitral annulus; MVC, mitral valve closure. \*Values are significantly different between pathological and control subjects,  $P < 0.001$ . Red line, organic mitral regurgitation; green line, controls.

**Table 4** Comparison of the functional parameters of MA between patients with OMR and controls

	OMR patients N = 52	Controls N = 52	P
MA fractional area change (%)	22.4 ± 5	28 ± 5	<0.001
AP diameter change (%)	14.4 ± 6.4	19.1 ± 6	<0.001
AL-PM diameter change (%)	10 ± 4.1	12 ± 4.5	0.023
MA displacement (mm)	10 ± 1.8	10 ± 1.7	0.270
MA displacement velocity (mm/s)	58 ± 15	50 ± 9	<0.001

OMR, organic mitral regurgitation.

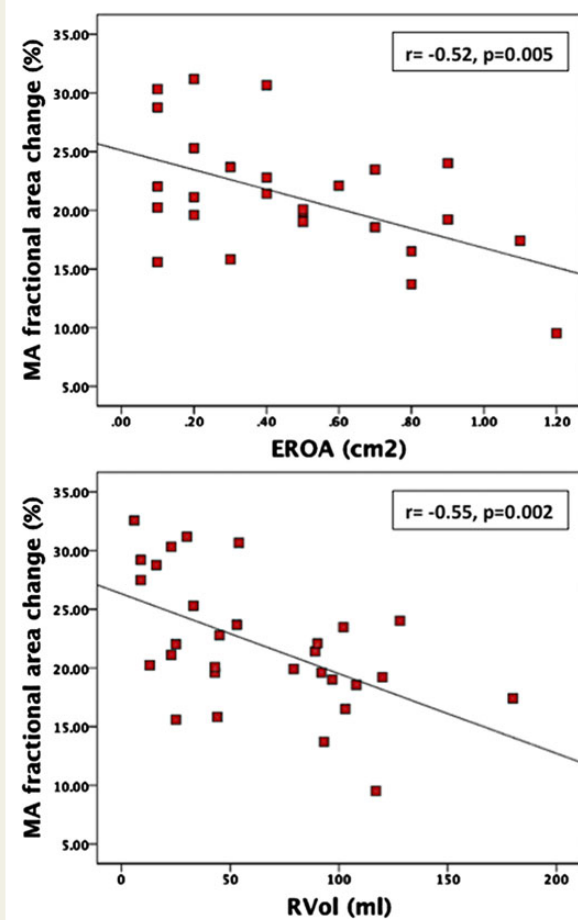


**Figure 4** Correlation between MA contractile dysfunction and OMR severity. EROA, effective regurgitant orifice area; MA, mitral annulus; RVol, regurgitant volume.

The increase of 37% in the MA area of our patients with OMR is lower than the increase of almost 80% in MA area from patients with OMR reported by Little et al.<sup>5</sup> However, the latter included only patients with at least moderate MR, while our study population

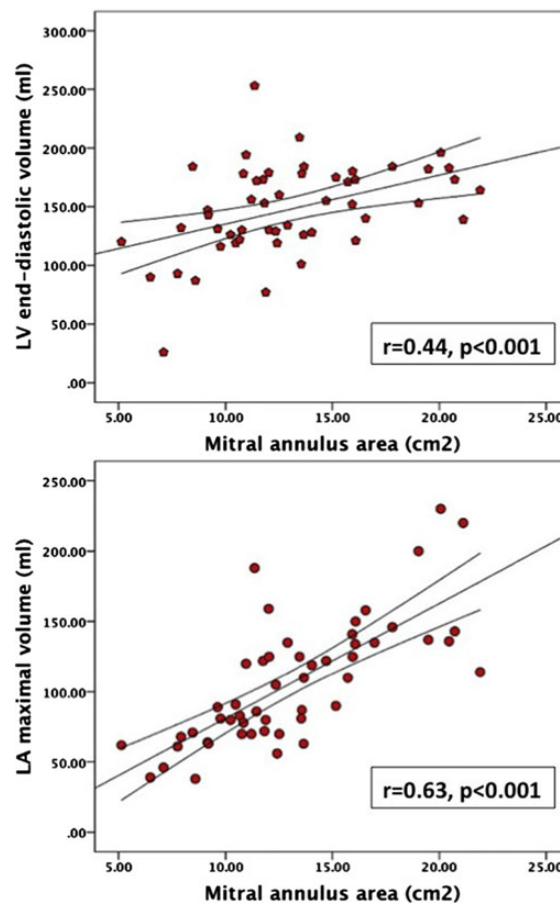


**Figure 5** MA relationships with the LA and LV volumes. LA, left atrium; LV, left ventricle.

enrolled patients with mild to severe OMR, with a significant proportion (25%) of patients mild MR.

Our patients with OMR presented larger MA size throughout the cardiac systole and decreased MA area contraction than controls. Grewal et al.,<sup>4</sup> using 3D transoesophageal echocardiography and a different software package to quantitate the MV, reported similar findings. Conversely, in a similar study that used 3D transthoracic echocardiography, Little et al.<sup>5</sup> reported that patients with MVP have MA remodelling but preserved MA dynamicity,<sup>5</sup> even though the MA fractional area change was relatively similar to the one obtained in our patients with OMR (21 ± 6 vs. 22 ± 5%).

Interestingly, in our patients with OMR, the reduced fractional area change of the MA was related to the severity of the MR. This is, from the best of our knowledge, the first study that correlates the extent of MA remodelling and dysfunction with the severity of OMR. Furthermore, we found that patients with a flail of the MV leaflet showed a further decrease in MA fractional area change, suggesting that the decreased MA shrinking during systole might have an additional negative impact on leaflet stress and chordae tension. Our data complete the results provided by Lee et al.,<sup>3</sup> which correlated the severity of the leaflet prolapse with the severity of MR.

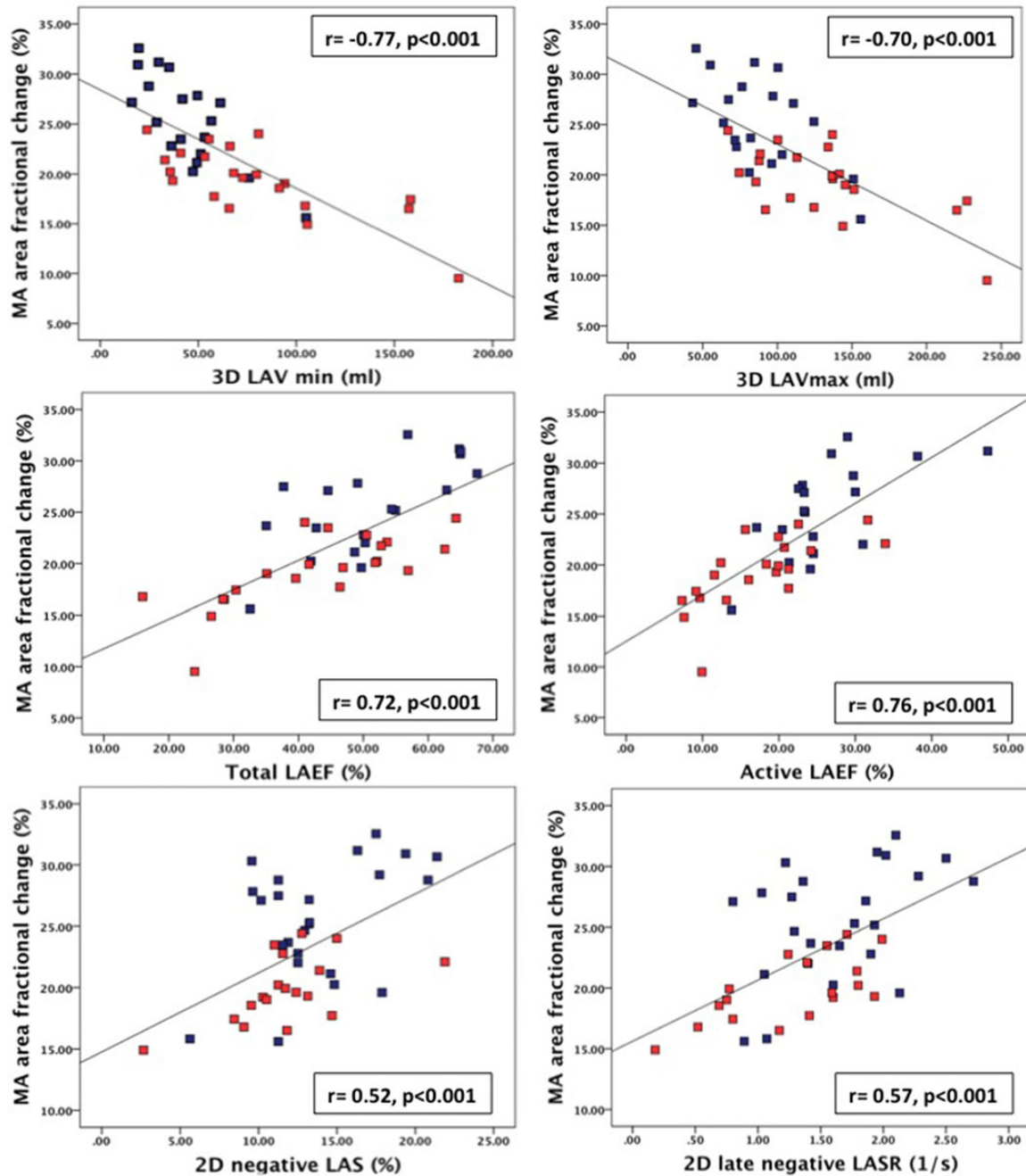


**Figure 6** Relationships between MA contractile function and LA size and function in patients with OMR. 3D, three dimensional; LAVmax, maximum left atrium volume; LAVmin, minimum left atrium volume; LAEF, left atrium emptying fraction; LAS, longitudinal atrial strain; LASR, longitudinal atrial strain rate; MA, mitral annulus.

Conversely, the extent of MA displacement was similar in patients with OMR and control subjects. These data are in accordance with the similar LV systolic function between the two groups. Conversely, Little *et al.*<sup>5</sup> found a lower MA displacement in patients with OMR than in controls ( $9 \pm 3$  vs.  $11 \pm 2$  mm). However, as mentioned above, the population from that study included patients with more severe degree of MR, so with a higher probability of having subclinical longitudinal LV dysfunction<sup>24</sup> due to chronic MR.

Even though patients with OMR presented relatively normal MA height and non-planarity angle at early-systole, the MA became progressively flatter from mid- to end-systole. MA non-planarity has been already reported to have a role in reducing MV leaflet stress.<sup>25</sup> The late systolic decrease in MA non-planarity can additionally increase leaflet stress in patients with OMR, with elongation and secondary chordae rupture.<sup>26</sup> As expected, MV tenting height and volume decreased from mid- to

**Table 5** Reproducibility for the MA parameters

n = 17	Reproducibility	
	Intra-observer (ICC)	Inter-observer (ICC)
AP diameter (cm)	0.97	0.89
AL-PM diameter (cm)	0.97	0.92
Commissural diameter (cm)	0.95	0.89
Circumference (cm)	0.97	0.92
Annular area (cm <sup>2</sup> )	0.98	0.95
ALA (cm <sup>2</sup> )	0.91	0.91
PLA (cm <sup>2</sup> )	0.90	0.88
Tenting height (mm)	0.89	0.91
Tenting volume (mL)	0.87	0.78

ICC, intra-class correlation.

end-systole in patients with OMR, due to the progressive mitral leaflet prolapse.

Even though MA remodelling and dysfunction seem to be related to the severity of OMR, their prognostic value and their relationships to left cardiac chamber size and function have received much less attention. Grewal *et al.*<sup>4</sup> showed that the patients with OMR present a loss of early MA contraction, despite the same magnitude of LV contraction, and suggested a *ventriculo-annular decoupling*. Based on our findings, we suggest that, in patients with OMR, the MA size and reduced fractional area shortening are more related to the LA than to LV size and dysfunction, at least at a stage of the disease when the LV still has a preserved ejection fraction.

LA dilation and dysfunction documented by 2D speckle-tracking analysis have recently been reported to be an additional good predictor of the need for surgery in patients with OMR.<sup>6</sup> Moreover, LA size has already been shown to have an independent role in functional MR.<sup>27</sup> Starting from our finding of a significant association between LA and MA function, future research will be needed to evaluate if, in addition to the LA function, the MA dysfunction might be a prognostic factor to be used for timing surgery in patients with OMR and the effects of LA size and function on recurrence of MR after successful MV repair. This hypothesis is also supported by the fact that the only significantly different characteristic between patients with and without MV flail was the decreased MA systolic contraction, which may suggest that a reduced extent of MA area reduction during systole can also be involved in the occurrence of chordae rupture.

An issue that remains to be addressed is which is the cause and which is the effect in the relation between the MA and the LA remodelling, in relation with the MR severity. MA intrinsic dysfunction was previously suggested in patients with MVP,<sup>28</sup> especially in the Barlow disease, and the disease progression was suggested to have a role in the recurrence of the MR post-operatively.<sup>17</sup> However, the presence of the MR leads to MA and LA remodelling, which further increase the severity of the MR. Therefore, a prospective long-term study designed to analyse the MA and the LA remodelling in patients with progressive OMR would likely clarify the cause–effect of this relationship.

## Study limitations

Our study documented an association between LA size and function and the extent of MA fractional area change in patients with OMR, without being able to specify if there is an actual cause–effect relation.

The need of multi-beat acquisition to achieve high temporal resolution limits the use of 3DE to patients with regular rhythm. Since many patients with MV disease show atrial fibrillation, the need of single-beat qualitative images is emerging as a clinical necessity to implement 3DE into the routine work-up of patients with MV disease.

In patients with mild MR, the CW-Doppler envelope of the regurgitant jet was not feasible for analysis due to a faint signal; therefore, the EROA and RVol could not be calculated in these patients. However, based on current guidelines recommendations, we used a multiparametric approach to assess the MR severity. Moreover, the EROA and RVol were calculated in all patients with more than mild MR, and used to separate between moderate and severe MR.

The software package used in this study performs MA tracking only during cardiac systole; therefore we were unable to analyse the MA dynamics during diastole. However, MA diastolic dynamics has been reported less accentuated and less important for the functional point of view.<sup>29</sup>

## Conclusions

Our study reveals that in patients with mild to severe OMR due to MVP or the Barlow disease, the extent of MA remodelling and dysfunction is related with MR severity, and the presence of MV leaflet flail. Moreover, MA remodelling and contractile dysfunction are associated with LA dilation and dysfunction, and not with the left ventricle dysfunction. Our findings of a direct relationship between MA remodelling and severity of OMR and between MA and LA dilation and dysfunction should foster new clinical researches aimed to clarify the role of the LA remodelling in identifying the correct timing for MV repair and the effects of LA size and function on recurrence of MR after successful MV repair.

**Conflict of interest:** L.P.B. and D.M. are consultants and received equipment grants from GE Vingmed and TomTec Imaging Systems. S.M. is an EACVI Research Grant winner on 2011 and an ESC Training Grant winner on 2014.

## Funding

An EACVI Research Grant won by S.M. in 2011 supported the research project.

## References

1. Freed LA, Levy D, Levine RA, Larson MG, Evans JC, Fuller DL *et al.* Prevalence and clinical outcome of mitral-valve prolapse. *N Engl J Med* 1999;**341**:1–7.
2. Iung B, Baron G, Butchart EG, Delahaye F, Gohlke-Barwolf C, Levang OW *et al.* A prospective survey of patients with valvular heart disease in Europe: The Euro Heart Survey on Valvular Heart Disease. *Eur Heart J* 2003;**24**:1231–43.
3. Lee AP, Hsiung MC, Salgo IS, Fang F, Xie JM, Zhang YC *et al.* Quantitative analysis of mitral valve morphology in mitral valve prolapse with real-time 3-dimensional echocardiography: importance of annular saddle shape in the pathogenesis of mitral regurgitation. *Circulation* 2013;**127**:832–41.
4. Grewal J, Suri R, Mankad S, Tanaka A, Mahoney DW, Schaff HV *et al.* Mitral annular dynamics in myxomatous valve disease: new insights with real-time 3-dimensional echocardiography. *Circulation* 2010;**121**:1423–31.

5. Little SH, Ben Zekry S, Lawrie GM, Zoghbi WA. Dynamic annular geometry and function in patients with mitral regurgitation: insight from three-dimensional annular tracking. *J Am Soc Echocardiogr* 2010;**23**:872–9.
6. Ring L, Rana BS, Wells FC, Kydd AC, Dutka DP. Atrial function as a guide to timing of intervention in mitral valve prolapse with mitral regurgitation. *JACC Cardiovasc Imaging* 2014;**7**:225–32.
7. Silbiger JJ. Novel pathogenetic mechanisms and structural adaptations in ischemic mitral regurgitation. *J Am Soc Echocardiogr* 2013;**26**:1107–17.
8. Ersboll M, Valeur N, Andersen MJ, Mogensen UM, Vinther M, Svendsen JH *et al*. Early echocardiographic deformation analysis for the prediction of sudden cardiac death and life-threatening arrhythmias after myocardial infarction. *JACC Cardiovasc Imaging* 2013;**6**:851–60.
9. Cameli M, Caputo M, Mondillo S, Ballo P, Palmerini E, Lisi M *et al*. Feasibility and reference values of left atrial longitudinal strain imaging by two-dimensional speckle tracking. *Cardiovasc Ultrasound* 2009;**7**:6.
10. Anyanwu AC, Adams DH. Etiologic classification of degenerative mitral valve disease: Barlow's disease and fibroelastic deficiency. *Semin Thorac Cardiovasc Surg* 2007;**19**:90–6.
11. Hayek E, Gring CN, Griffin BP. Mitral valve prolapse. *Lancet* 2005;**365**:507–18.
12. Lancellotti P, Tribouilloy C, Hagendorff A, Popescu BA, Edvardsen T, Pierard LA *et al*. Recommendations for the echocardiographic assessment of native valvular regurgitation: an executive summary from the European Association of Cardiovascular Imaging. *Eur Heart J Cardiovasc Imaging* 2013;**14**:611–44.
13. Muraru D, Badano LP, Peluso D, Dal Bianco L, Casablanca S, Kocabay G *et al*. Comprehensive analysis of left ventricular geometry and function by three-dimensional echocardiography in healthy adults. *J Am Soc Echocardiogr* 2013;**26**:618–28.
14. Mor-Avi V, Yodwut C, Jenkins C, Kuhl H, Nesser HJ, Marwick TH *et al*. Real-time 3D echocardiographic quantification of left atrial volume: multicenter study for validation with CMR. *JACC Cardiovasc Imaging* 2012;**5**:769–77.
15. Mihaila S, Muraru D, Piasentini E, Miglioranza MH, Peluso D, Cucchini U *et al*. Quantitative analysis of mitral annular geometry and function in healthy volunteers using transthoracic three-dimensional echocardiography. *J Am Soc Echocardiogr* 2014;**27**:846–57.
16. Mohty D, Orszulak TA, Schaff HV, Avierinos JF, Tajik JA, Enriquez-Sarano M. Very long-term survival and durability of mitral valve repair for mitral valve prolapse. *Circulation* 2001;**104**(12 Suppl. 1):I1–7.
17. Flameng W, Meuris B, Herijgers P, Herregods MC. Durability of mitral valve repair in Barlow disease versus fibroelastic deficiency. *J Thorac Cardiovasc Surg* 2008;**135**:274–82.
18. Adams DH, Anyanwu AC, Rahmanian PB, Abascal V, Salzberg SP, Filsoufi F. Large annuloplasty rings facilitate mitral valve repair in Barlow's disease. *Ann Thorac Surg* 2006;**82**:2096–100; discussion 101.
19. Zoghbi WA, Enriquez-Sarano M, Foster E, Grayburn PA, Kraft CD, Levine RA *et al*. Recommendations for evaluation of the severity of native valvular regurgitation with two-dimensional and Doppler echocardiography. *J Am Soc Echocardiogr* 2003;**16**:777–802.
20. Lancellotti P, Moura L, Pierard LA, Agricola E, Popescu BA, Tribouilloy C *et al*. European Association of Echocardiography recommendations for the assessment of valvular regurgitation. Part 2: mitral and tricuspid regurgitation (native valve disease). *Eur J Echocardiograph* 2010;**11**:307–32.
21. Foster GP, Dunn AK, Abraham S, Ahmadi N, Sarraf G. Accurate measurement of mitral annular dimensions by echocardiography: importance of correctly aligned imaging planes and anatomic landmarks. *J Am Soc Echocardiogr* 2009;**22**:458–63.
22. Mahmood F, Subramaniam B, Gorman JH 3rd, Levine RM, Gorman RC, Maslow A *et al*. Three-dimensional echocardiographic assessment of changes in mitral valve geometry after valve repair. *Ann Thorac Surg* 2009;**88**:1838–44.
23. Biaggi P, Jedrzkiewicz S, Gruner C, Meineri M, Karski J, Vegas A *et al*. Quantification of mitral valve anatomy by three-dimensional transesophageal echocardiography in mitral valve prolapse predicts surgical anatomy and the complexity of mitral valve repair. *J Am Soc Echocardiogr* 2012;**25**:758–65.
24. Enriquez-Sarano M, Tajik AJ, Schaff HV, Orszulak TA, Bailey KR, Frye RL. Echocardiographic prediction of survival after surgical correction of organic mitral regurgitation. *Circulation* 1994;**90**:830–7.
25. Salgo IS, Gorman JH 3rd, Gorman RC, Jackson BM, Bowen FW, Plappert T *et al*. Effect of annular shape on leaflet curvature in reducing mitral leaflet stress. *Circulation* 2002;**106**:711–7.
26. Jensen MO, Jensen H, Levine RA, Yoganathan AP, Andersen NT, Nygaard H *et al*. Saddle-shaped mitral valve annuloplasty rings improve leaflet coaptation geometry. *J Thorac Cardiovasc Surg* 2011;**142**:697–703.
27. Gertz ZM, Raina A, Saghy L, Zado ES, Callans DJ, Marchlinski FE *et al*. Evidence of atrial functional mitral regurgitation due to atrial fibrillation: reversal with arrhythmia control. *J Am Coll Cardiol* 2011;**58**:1474–81.
28. Mohty D, Enriquez-Sarano M. The long-term outcome of mitral valve repair for mitral valve prolapse. *Curr Cardiol Rep* 2002;**4**:104–10.
29. Kwan J, Jeon MJ, Kim DH, Park KS, Lee WH. Does the mitral annulus shrink or enlarge during systole? A real-time 3D echocardiography study. *J Korean Med Sci* 2009;**24**:203–8.